Characterization Of a G Protein α Subunit Encoded Gene From The Dimorphic Fungus-*Tremella Fuciformis*

Hanyu Zhu
Hengyang Normal University
Dongmei Liu
Huazhong Agricultural University
Liesheng Zheng
Huazhong Agricultural University
Liguo Chen
Huazhong Agricultural University
Aimin Ma (aiminma@mail.hzau.edu.cn)
Huazhong Agricultural University https://orcid.org/0000-0003-4728-1201

Research Article

Keywords: Tremella fuciformis, dimorphism, G protein α subunit, gene function, morphological change

Posted Date: June 18th, 2021

DOI: https://doi.org/10.21203/rs.3.rs-586507/v1

Abstract

Tremella fuciformis is a dimorphic fungus which can undertake the reversible transition between yeast and pseudohypha forms. G protein α subunit (Gα) carries different signals to regulate a variety of biological processes in eukaryotes, including fungal dimorphism. In this study, a novel Gα subunit encoded gene, *TrGpa1*, was firstly cloned from *T. fuciformis*. The *TrGpa1* open reading frame has 1059 nucleotides, and encodes a protein which belongs to the group I of $G\alpha_i$ superfamily. Furthermore, the role of *TrGpa1* in the *T. fuciformis* dimorphism was analysed by gene overexpression and knockdown. Stable integration of the target gene into the genome was confirmed by PCR and Southern blot hybridization. Transformants with the highest and lowest *TrGpa1* expression levels were selected via quantitative real-time PCR analysis and Western blot. Each transformant was compared with the wild-type strain about the morphological change under different environmental factors, including pH values, temperature, cultural time, inoculum size, and quorum-sensing molecules (farnesol and tyrosol). Comparing with the wild-type strain, the overexpression transformant always had higher ratios of pseudohyphae, while the knockdown transformant had less proportions of pseudohyphae. Therefore, the *TrGpa1* involves in the dimorphism of *T. fuciformis* and plays a positive role in promoting pseudohyphal growth.

Introduction

The heterotrimeric guanine nucleotide-binding proteins (G proteins), universal signaling proteins in eukaryotes, carry different signals from the receptors to various effectors, then regulate a variety of biological processes (Kang et al. 2011). The G proteins are highly conserved, and consist of Gα, Gβ and Gγ subunits. In the inactive state, these three subunits are tightly associated together. Once the Gα subunit was activated by G protein-coupled receptors (GPCRs), G protein dissociates to form Gα and Gβ-Gγ dimeric subunits. Each of them can interact with downstream effectors, which subsequently trigger a series of intracellular responses (Perez-Sanchez et al. 2010; Valle-Maldonado et al. 2015).

Fungal dimorphism is an intriguing morphological transition, which undertakes a morphological interconversion between the yeast form and the mycelial/pseudohypha form (Nickerson and Atkin 2017). This switch promotes the disease progression in the pathogenic filamentous species, which is necessary for the invasion to hosts and the expression of virulence factors (Wilson et al. 2010; Boyce and Andrianopoulos 2015). Lots of researches showed Gα subunits had linkage with morphological transition in dimorphic fungi. For *Ustilago maydis*, the yeast colonies of *cap1*-defective cells failed to form filamentous colonies, which resulted in a significantly decreased pathogenicity (Takach and Gold 2010). In *Sporothrix schenckii*, Gα subunits SSG-1 and SSG-2 involved in the dimorphism and pathogenicity (Pérez-Sánchez et al. 2010; Yemelin et al. 2017). The Δ*MgGpa3* mutant of *Mycosphaerella graminicola* showed more pronounced yeast-like growth accompanied with hampered filamentation, which suppressed the transition from yeast-like form to filamentous form (Orton et al. 2011). As to *Mucor circinelloides*, the *gpa3* expression levels was decreased during the dimorphic transition from mycelium to yeast cell (Patiño-Medina et al. 2019). In *Candida albicans*, the Gpa2 played an important role in the yeast-hypha dimorphic transition in the response of *C. albicans* to some environmental inducers

(Wilson et al. 2010). The Δ*gpa2* mutant strains of *Saccharomyces cerevisiae* had a defect in pseudohyphal growth, while constitutive overexpression of *gpa2* stimulated filamentation of mutant (Kayikci and Magwene 2018).

Tremella fuciformis, or white jelly mushroom, is a typical dimorphic fungus having the yeast-hypha and yeast-pseudohypha transition triggered by environmental cues (Hou et al. 2011). Previous studies about the *T. fuciformis* dimorphism mainly focused on the environmental factors which affected its dimorphism and cell wall polysaccharides changes during dimorphic transition (Zhu et al. 2016). Little is known about the functions of signaling proteins during the dimorphic change of *T. fuciformis*. In the present study, a Gα subunit gene (*TrGpa1*) was cloned and characterized its contributions to the *T. fuciformis* dimorphism. The gene overexpression and knockdown vectors were constructed to evaluate its roles in the dimorphic transition in response to the environmental inducers.

Materials And Methods

Strains and Culture Conditions

The *T. fuciformis* haploid yeast-like cell Y32, was maintained in the Laboratory of Food Microbiology, Huazhong Agricultural University, and subcultured on potato dextrose agar (Difco, Detroit, MI, USA) slants. The LM medium (20 g·L^{-1} glucose, 1.32 g·L^{-1} $(NH_4)_2SO_4$, 0.25 g·L^{-1} $MgSO_4 \cdot 7H_2O$, 0.5 g·L^{-1} $KH_2PO_4 \cdot 3H_2O$, 0.2 mg·L^{-1} vitamin B_1, 2 mg·L^{-1} $ZnSO_4 \cdot 7H_2O$, and 0.5 g·L^{-1} $CaCl_2 \cdot 2H_2O$) was designed for strain culturing. The strains were incubated at 25°C using an orbital shaker (Fuma, Shanghai, China) at 150 rpm. *Escherichia coli* DH5α (Takara, Dalian, China) was used as a host for vectors' cloning and propagation. The *Agrobacrerium tumefaciens* strain EHA105 (Invitrogen, Shanghai, China), grown in YEB medium (Sigma-Aldrich, Shanghai, China) with the selective antibiotics (50 μg·mL^{-1} rifampicin and 100 μg·mL^{-1} kanamycin), was used to transform Y32. The *T. fuciformis* transformants were selected by PDSA (PDA containing 50 μg·mL^{-1} hygromycin and 200 μg·mL^{-1} cefotaxime sodium).

Full-length Gene Cloning and Bioinformatical Analysis

Gα subunit gene, named as *TrGpa1*, and the DNA (GenBank accession no. MH091706) and cDNA (GenBank accession no. MH101517) were acquired in our previous work. Total RNA and DNA were extracted from Y32 strain using the RNaiso^{TM} plus (Takara, Dalian, China) and the cetyltrimethylammonium bromide (CTAB) method (Yin et al. 2015), respectively. The *TrGpa1* was cloned by PCR with the specific primers listed on Table 1. The amplification procedures were carried out as follows: an initial denaturation at 94°C for 5 min; 35 cycles of 94°C denaturation for 30 s, 60°C annealing for 30 s, 72°C elongation for 90 s; and a final extension at 72°C for 10 min.

Table 1 Primers for PCR amplification in this work.

Names	Sequences (5'→3')	Descriptions
TrGpa1-F	CATGGGGTGCACACAGTCG	Primers for *TrGpa1*
TrGpa1-R	TCAAAGCAATCCGACCTCCC	
OE-F	CCTAGGATGGGGTGCACACAG	Primers for *TrGpa1* overexpression
OE-R	TTCGAATCAAAGCAATCCG	
F-F	ACGCGTGGAACGAGATCAAGATGCTC	Amplify a sense fragment for the RNAi vector
F-R	CCTAGGCGTGCACGGAGGATGTCTTGG	
R-F	CCTAGGGGACCGCCGGGTCCTGCCAC	Amplify an antisense fragment for the RNAi vector
R-R	TTCGAAGGAACGAGATCAAGATGCTC	
EH-F	GCAGAAGAACGGCATCAAGGTG	Detects the eGFP and hygromycin expression
EH-R	CAGGCTCTCGCTAAACTCCCC	
qGpa1-F	CCGCCTTGGTCTTCCTCATT	*TrGpa1* primers for qRT-PCR
qGpa1-R	TAGTTGCTCCCGCCCTTGTA	
tubulin-F	GATGACCATTTCTTGCTTC	Tubulin primers for qRT-PCR
tubulin-R	GTTCTGACATTTGCTACCG	
M13-F	CGCCAGGGTTTTCCCAGTCACGAC	Primers for sequencing
M13-R	AGCGGATAACAATTTCACACAGGA	

The recognition sequences for restriction enzyme are underlined.

Bioinformation analysis of *TrGpa1* was performed by following steps. The amino acid sequence was deduced by Translate tool (http://web.expasy.org/translate/). The theoretical isoelectric point and molecular weight were predicted using Compute pI/Mw (http://expasy.org/tools/protparam.html). The conserved domains were identified from the National Center for Biotechnology Information (NCBI) (http://www.ncbi.nlm.nih.gov/Structure/cdd/wrpsb.cgi). Sequence similarity was analysed using Basic Local Alignment Search Tool (BLAST) at the NCBI (https://blast.ncbi.nlm.nih.gov/Blast.cgi). Multi-sequence alignment was generated using ClustalW (http://www.clustal.org/). The phylogenetic tree was constructed using neighbor joining method implemented in Molecular Evolutionary Genetics Analysis (MEGA) version 6 program.

Vector Construction and *Agrobacterium*-mediated Transformation

The overexpression and knockdown vectors of *TrGpa1* were constructed according to the vector pGEH-GH (Zhu et al. 2017) based on pCAMBIA 1302 backbone (Cambia, Brisbane, Australia). The *TrGpa1* amplified using the primers with *Mlu*I and *Asu*II restriction sites were digested and introduced into pGEH-GH to generate the overexpression vector pTrGpa1-OE (Fig. 1a). The knockdown vector (pTrGpa1-OE) was generated by the ligation of a 439 bp fragment (flanking *Mlu*I and *Bln*I restriction sites) and a 325 bp (flanking *Bln*I and *Asu*II restriction sites) fragments. The plasmid was expected to encode a hairpin RNA included two 325 bp complementary regions separated by a 124 bp spacer fragment (Fig. 1b).

All vectors were transformed into the *A. tumefaciens* strain EHA105 component cells. *Agrobacterium*-mediated transformation of *T. fuciformis* Y32 cells were performed according to previous work (Zhu et al. 2017). The transformants were subcultured for five rounds on PDSA, then the total DNA were extracted. The existence of enhanced green fluorescent protein gene (*egfp*)-hygromycin B phosphotransferase gene (*hph*) fusion gene was assessed by PCR using primers EH-F and EH-R. The integration of genes in the genome was analysed by Southern blot with digoxigenin (Roche Diagnostics, Mannheim, Germany) labeled *hph*. DNA of Y32 was used as the negative control, and plasmid of pGEH-GH was applied as the positive control. Transformants were measured by using a fluorescence microscope (DM 6000 B, Leica Microsystems, Germany) to analyze the *egfp* expression. The images were captured under 40 × objective and samples were measured with a green fluorescence filter (546 nm).

Gene Expression Analysis

Total RNA was extracted and reverse transcribed (*TransScript*® first-strand cDNA synthesis supermix, Transgen, China) according to the manufacturer's protocol. Quantitative real-time PCR (qRT-PCR) was performed on the ABI ViiA7 Real-Time PCR System (Applied Biosystems, USA) according to the manufacturer's protocol (Takara), using *β-tubulin* as the endogenous control. The primer sequences for the qRT-PCR of *TrGpa1* and *β-tubulin* are listed on Table 1. The qRT-PCR conditions were 95°C for 10 min, followed by 30 cycles of 95°C for 30 s, and 60°C for 30 s. The expression ratios were calculated according to the $2^{-\triangle\triangle Ct}$ method and each qRT-PCR reaction was carried out in triplicate independently. Data were analysed by one-way analysis of variance (ANOVA), followed by Ducan's multiple range tests using SPSS 26.0 software.

Transformants selected based on the qRT-PCR assays and Y32 were performed with Western blots. Cells were lysed in buffer containing protease and phosphatase inhibitor cocktails (Sigma, St. Louis, MO, USA). Then total protein content was measured with BCA Protein Assay Kit according to the manufacturer's protocol, and 40 μg of proteins were separated on 10% SDS polyacrylamide gels and transferred to PVDF membrane (Thermo Fisher Scientific, USA) using a Semi Dry Blotter (Thermo Fisher Scientific, USA) for 1 h at 20 volts. After blocking with TBST buffer (5% dry milk powder in tris-buffered saline and Tween 20) for 1 h, the membrane was incubated with the primary rabbit antibodies against TrGpa1 at 4°C overnight. After 5 washing steps with TBST buffer, blots were incubated with the secondary antibodies: anti-rabbit IgG in the dilution of 1:2000 in 5% milk/TBST at room temperature for 2 h. The membranes were performed using the SuperSignal ECL Solution for Western blot (Willget Biotech, Shanghai, China).

Densitometric evaluation was performed with ImageJ software (National Institute of Health, New York, NY).

Phenotypic Analysis

The sub-cultured cells in LM medium were aseptically collected by centrifugation at 5000 × *g* for 5 min, washed three times and distributed in 50 mL of medium to obtain final concentration of 10^5 cells·mL^{-1}. Except the given situations, the 50 mL of LM medium containing cells were incubated at 25°C on an orbital shaker at pH 7 for 3 to 5 d. The pH of the medium was adjusted by the addition of dibasic phosphate-citric acid buffer to the desired pH value.

The transformants and Y32 were cultured under different conditions to test the morphological changes in Y32 and transformants. 20°C, 25°C, 28°C, 30°C, 37°C were chosen as the temperature parameters and 3, 4, 5, 6, 7, 8 as the pH parameters. The cells were incubated for 2 to 9 d for the culture time parameters. Each LM medium containing different concentrations of cells (10^3, 10^4, 10^5, 10^6, and 10^7 cells·mL^{-1}) was cultured respectively. Quorum sensing molecules (QSMs) including farnesol and tyrosol (Sigma, USA) in different concentrations (5, 25, 50, 100, 200 μmol·L^{-1}) were also prepared to observe their effects on morphological changes. Strains supplemented with 1% methanol were the controls for each assay. All experiments were performed in triplicate of each treatment. Data were analysed by ANOVA, followed by Ducan's multiple range tests.

Samples were observed at 20 × objective by an optical microscope (Leica, Germany). Three or more cells connected at the end of the long axes or in a definite direction or an elongated cell with a daughter cell and an ellipsoidal cell having two branched daughter cells were counted as a pseudohypha. Only differentiated cells were quantified and normalized to 100% (yeast/pseudohypha cells). For each repetition, at least 300 cells were counted under the microscopy.

Results

The Bioinformation Analysis of *TrGpa1*

The DNA sequence of *TrGpa1* is 1436 bp and contains eight introns of 53, 61, 41, 40, 45, 47, 46, and 44 nucleotides, respectively (data not shown). The 5' and 3' borders of the eight introns showed the same splicing sites (GT-AG) which are the common sequences for introns of filamentous fungi (Yin et al. 2015). The CDs encoded a protein of 352 amino acid residues. The calculated theoretical isoelectric point of TrGpa1 was 5.55, and the molecular weight was 40.18 kDa. The conserved domain analysis of the amino acid sequence revealed that TrGpa1 contained the GTPase domain (G1-G5), an ATP/GTP binding regions (G/AXXXXGKT/S), and the βγ complex interaction site.

Multiple sequence alignment of the predicted amino acid sequence of TrGpa1 with eight known fungal Gα subunits available in NCBI database was performed by ClustalW program. The results revealed that TrGpa1 had highly identities with other homologues from *Kwoniella heveanensis* (89%, OCF36875.1),

Cryptococcus gattii (86%, XP_003191999.1), *C. neoformans* (86%, XP_566528.1), *Pisolithus sp.* (66%, AAK15759.1), *Schizophyllum commune* (66%, XP_003029155.1), *Laccaria bicolor* (65%, XP_001888946.1), *Lentinula edodes* (65%, AAP13579.1), *Hypsizygus marmoreus* (65%, KYQ31721.1) (Fig. 2).

A phylogenetic tree was constructed based on the multiple sequence alignments with the Gα subunits from other species (Fig. 3). The Gα proteins were divided into four groups according to their evolutionary relationships. It revealed that TrGpa1 belongs to the group I of mammalian $G\alpha_i$ superfamily. The amino acid sequence of TrGpa1 contained the consensus myristoylation site, indicated as MGXXXS at the N terminus, but did not present a consensus CXXX sequence (pertussis toxin-catalyzed ADP-ribosylation site) at the C terminus (Fig. 2).

Stability Test of Transformants

Single colonies of *T. fuciformis* transformants were selected randomly and sub-cultured in PDSA. To confirm the integration of the overexpression and knockdown fragments, the DNA was extracted from 12 randomly selected transformants, and Y32. Amplification of a 500 bp DNA product, suggesting that the *egfp-hph* fusion gene had been transferred into these transformants (Fig. 4a). Southern blot analysis performed in 10 PCR positive transformants showed that all transformants except one appeared to have copies of the *hph* gene at random sites, but Y32 showed no hybridization (Fig. 4b). The transformants were inspected by fluorescence microscopy, respectively. It showed stable and highly efficient eGFP expression in the individual transformants (Fig. 5).

Gene Expression Analysis of Transformants

The qRT-PCR assays were used to test the expression of *TrGpa1*. For the overexpression transformants (Fig. 6a), the expression level increased from 1.5 to 2.5 folds, and the transformant with the highest relative mRNA level was selected and sub-cultured. In addition, the gene suppression ratio ranged from 52.10% to 68.26% among the knockdown transformants (Fig. 6a). Thus, the transformant having the highest gene suppression ratio was chosen. Then Western blot was subsequently undertaken in Y32 and transformants with the maximum and minimum expression level. As shown in Fig 6b, TrGpa1 in the overexpression transformants was expressed at a higher level than Y32, whereas at a lower level in the knockdown transformants, which is in accordance with the qRT-PCR analysis.

TrGpa1 Contributes to *T. fuciformis* Dimorphism

The dimorphic-related functions of *TrGpa1* were characterized. It was shown that the *TrGpa1* was required for pseudohyphal differentiation of *T. fuciformis*. When the environmental conditions change, the transition from yeast to pseudohypha in Y32, the overexpression and knockdown transformants were influenced by the environmental factors, including pH, temperature, inoculum size, culture time, farnesol and tyrosol concentration (Fig. 7). Comparing with Y32, the overexpression transformant always had

higher ratios of pseudohyphae, and the knockdown transformant always had less proportions of pseudohyphae (Fig. 7).

Discussion

The dimorphism is a reversible transition and depends upon the environment to which the fungi are exposed (Wang et al. 2020). *T. fuciformis*, an edible jelly mushroom, has the capacity to perform this type of morphogenesis (Zhu et al. 2016). It has been demonstrated that G proteins are key regulators of this morphological transition in many dimorphic fungi (Park et al. 2020). However, G proteins and their functions that are involved in *T. fuciformis* have been little known.

In this work, we have cloned the *TrGpa1*, a gene encoded Gα subunit from *T. fuciformis*. Filamentous fungi usually have three Gα-encoded genes that belong to three groups. According to the phylogenetic tree, TrGpa1, the *TrGpa1* expressed protein, belongs to the group I of $G\alpha_i$ superfamily containing the characteristic sequence sites (Fig. 3). The site for myristoylation at the N terminus is important to attachment to the GPCRs in membrane (Li et al. 2019). The amino acid sequence of TrGpa1 did not contain the conserved pertussis toxin site at the C terminus. ADP ribosylation of the $G\alpha_i$ subunits locks the activity of G proteins and prevents the activation by GPCRs (Appleton et al. 2014).

Furthermore, the overexpression and knockdown vectors were constructed for identifying the function of *TrGpa1*. Since the gene knockout methods are lacking in *T. fuciformis*, RNA interference (RNAi) was performed for identifying the function of *TrGpa1* (Wang et al. 2017). Though it causes only partial gene silencing, RNAi technology provides variable rates of gene suppression transformants. Therefore, it makes the possibility to investigate the effects of genes on the phenotypes of interest and the minimum effective inhibition rate. For example, in *Magnaporthe oryzae*, only a slight decrease in the expression of some calcium signaling related genes caused a complete loss of infection-related morphogenesis and pathogenicity (Lange and Peiter 2020). Nevertheless, strong knockdown of hydrophobin gene *Mpg1* did not severely affect its pathogenicity, despite knockout of this gene presented a drastic reduction in pathogenicity (Han 2018). Thus, the impacts on the phenotypes would differ among different genes. Here we only chose the transformant with the highest or lowest gene expression. It is worthy of discussion how the rates of gene suppression contribute to the dimorphic phenotypes in our future work.

The characterization of dimorphic related functions indicated that *TrGpa1* played a positive role in the promotion of pseudohyphal growth. The overexpression of *TrGpa1* enhances the response to different conditions and promotes the pseudohyphal formation. Cells lacking TrGpa1 have a defect in pseudohyphal development in response to specific environmental cues. For dimorphic fungi, cell morphology is depending on the inoculation size. There is a general phenomenon for all dimorphic fungi (Wedge et al. 2016), that is when inoculation at $\geq 10^6$ cells·mL^{-1}, budding yeasts are produced, while pseudohyphae and mycelia are produced following inoculation at $\leq 10^6$ cells·mL^{-1}. In the present study, interestingly, the overexpression transformant had high ratios of pseudohyphae, even when the inoculum size was larger than 10^6 cells·mL^{-1} (Fig. 7c). In addition to the inoculation size, extracellular

QSMs contribute to *T. fuciformis* dimorphism. In *C. albicans*, farnesol is a characterized QSM, which suppresses filamentous formation. Tyrosol, another QSM produced by *C. albicans*, stimulates the yeast-to-hypha conversion (Han et al. 2011; Monteiro et al. 2017). In Y32 and the transformants, farnesol and tyrosol played the same roles. Farnesol effectively blocked the transition from yeast to pseudohypha at the concentration of 50 μmol·L^{-1} (Fig. 7e), while tyrosol stimulated this transition (Fig. 7f). The pseudohyphae ratios of knockdown transformant were largely decreased in the addition of farnesol, while the pseudohyphae ratios of overexpression transformant were slightly decreased, which shows the overexpression transformant was less sensitive to the QSMs (Fig. 7).

However, the TrGpa1 involved signal pathways still remains a mystery. Former studies showed many Gα subunits are involved in the cAMP-protein kinase A (PKA) and the mitogen-activated protein kinase (MAPK) pathways (Nogueira et al. 2015; Shwab et al. 2017; Martínez-Soto et al. 2020). Here the exogenous addition of cAMP (10 mmol·L^{-1}) had no apparent influences on the yeast-pseudohypha transition, indicates *TrGpa1* may not involve in the cAMP/PKA pathway (data not shown).

In conclusion, a G protein α subunit encoded gene *TrGpa1*, was cloned from the dimorphic fungus *T. fuciformis*. The *TrGpa1* encoded a protein of 352 amino acid residues and the TrGpa1 belongs to the group I of $G\alpha_i$ superfamily. The function of *TrGpa1* was characterized by gene overexpression and knockdown. The results have demonstrated that *TrGpa1* involved in *T. fuciformis* dimorphism and supports a positive role in the transition from yeast to pseudohyphal growth under different environmental conditions. In our future study, the pathways *TrGpa1* involved in and rates of gene suppression need to be further investigated.

Declarations

Author Contributions H.Z. and A.M. designed the study; L.Z. and L.C. collected the samples; H.Z. and D.L. performed the laboratory work; H.Z. performed the data analysis and wrote the manuscript; A.M., L.Z., and L.C. reviewed and revised the writing.

Funding This work was supported by grants from the National Natural Science Foundation of China (NSFC) (No. 30972072 and No. 31572182) to Aimin Ma and from the General project of Hunan Provincial Education Department (No. 19C0289) to Hanyu Zhu.

Availability of data and materials The DNA and cDNA sequences of *TrGpa1* can be downloaded from the National Center for Biotechnology Information (NCBI), and the GenBank accession numbers are MH091706 and MH101517.

Compliance with ethical standards

Conflicts of Interest The authors declare no conflicts of interest.

Ethical statement This article does not contain any studies with human participants or animals performed by any of the authors.

Consent for publication All authors read and approved the final version of the manuscript.

References

1. Appleton KM, Bigham KJ, Lindsey CC, Hazard S, Lirjoni J, et al (2014) Development of inhibitors of heterotrimeric $G\alpha_i$ subunits. Bioorg Med Chem 22:3423-3434
2. Boyce KJ, Andrianopoulos A (2015) Fungal dimorphism: the switch from hyphae to yeast is a specialized morphogenetic adaptation allowing colonization of a host. FEMS Microbiol Rev 39:797-811
3. Han H (2018) RNA Interference to knock down gene expression. Methods Mol Biol 1706:293-302
4. Han TL, Cannon RD, Villasbôas SG (2011) The metabolic basis of *Candida albicans* morphogenesis and quorum sensing. Fungal Genet Biol 48:747-763
5. Hou LH, Chen Y, Ma CJ, Liu J, Chen LG et al (2011) Effects of environmental factors on dimorphic transition of the jelly mushroom *Tremella fuciformis*. Cryptogam Mycol 32:421-428
6. Kang GJ, Gong ZJ, Cheng JA, Zhu ZR, Mao CG (2011) Cloning and expression analysis of a G-protein α subunit-$G\alpha_o$ in the rice water weevil *Lissorhoptrus oryzophilus* Kuschel. Arch Insect Biochem Physiol 76:43-54
7. Kayikci Ö, Magwene PM (2018) Divergent roles for cAMP-PKA signaling in the regulation of filamentous growth in *Saccharomyces cerevisiae* and *Saccharomyces bayanus*. G3 (Bethesda) 8:3529-3538
8. Lange M, Peiter E (2020) Calcium transport proteins in fungi: the phylogenetic diversity of their relevance for growth, virulence, and stress resistance. Front Microbiol 10:3100
9. Li X, Zhong KL, Yin ZY, Hu JX, Wang WH, et al (2019) The seven transmembrane domain protein MoRgs7 functions in surface perception and undergoes coronin MoCrn1-dependent endocytosis in complex with Gα subunit MoMagA to promote cAMP signaling and appressorium formation in *Magnaporthe oryzae*. PLoS Pathog 15:e1007382
10. Martínez-Soto D, Ortiz-Castellanos L, Robledo-Briones M, León-Ramírez CG (2020) Molecular mechanisms involved in the multicellular growth of *Ustilaginomycetes*. Microorganisms 8:1072
11. Nickerson KW, Atkin AL (2017) Deciphering fungal dimorphism: farnesol's unanswered questions. Mol Microbiol 103:567-575
12. Monteiro DR, Arias LS, Fernandes RA, Deszo da Silva LF, de Castilho MOVF et al (2017) Antifungal activity of tyrosol and farnesol used in combination against *Candida* species in the planktonic state or forming biofilms. J Appl Microbiol 123:392-400
13. Nogueira KM, Costa MN, de Paula RG, Mendonça-Natividade FC, Ricci-Azevedo R et al (2015) Evidence of cAMP involvement in cellobiohydrolase expression and secretion by *Trichoderma reesei*

in presence of the inducer sophorose. BMC Microbiol 15:195

14. Orton ES, Deller S, Brown JK (2011) *Mycosphaerella graminicola*: from genomics to disease control. Mol Plant Pathol 12:413-424
15. Park HS, Kim MJ, Yu JH, Shin KS (2020) Heterotrimeric G-protein signalers and RGSs in *Aspergillus fumigatus*. Pathogens 9:902
16. Patiño-Medina JA, Reyes-Mares NY, Valle-Maldonado MI, Jácome-Galarza IE, Pérez-Arques C et al (2019) Heterotrimeric G-alpha subunits Gpa11 and Gpa12 define a transduction pathway that control spore size and virulence in *Mucor circinelloides*. PLoS One 14:e0226682
17. Pérez-Sánchez L, González E, Colón-Lorenzo EE, González-Velázquez W, González-Méndez R et al (2010) Interaction of the heterotrimeric G protein alpha subunit SSG-1 of *Sporothrix schenckii* with proteins related to stress response and fungal pathogenicity using a yeast two-hybrid assay. BMC Microbiol 19:262
18. Shwab EK, Juvvadi PR, Waitt G, Soderblom EJ, Moseley MA et al (2017) Novel phosphoregulatory switch controls the activity and function of the major catalytic subunit of protein kinase A in *Aspergillus fumigatus*. mBio 8:e02319-02316
19. Takach JE, Gold SE (2010) Identification and characterization of Cap1, the adenylate cyclase-associated protein (CAP) ortholog in *Ustilago maydis*. Physiol Mol Plant Pathol 75:30-37
20. Valle-Maldonado MI, Jácome-Galarza IE, Díaz-Pérez AL, Martínez-Cadena G, Campos-García J et al (2015) Phylogenetic analysis of fungal heterotrimeric G protein-encoding genes and their expression during dimorphism in *Mucor circinelloides*. Fungal Biol 119:1179-1193
21. Wang S, Chen H, Tang X, Zhang H, Chen W et al (2017) Molecular tools for gene manipulation in filamentous fungi. Appl Microbiol Biotechnol 101:8063-8075
22. Wang YY, Wei XL, Bian ZY, Wei JC, Xu JR (2020) Coregulation of dimorphism and symbiosis by cyclic AMP signaling in the lichenized fungus *Umbilicaria muhlenbergii*. Proc Natl Acad Sci USA 117:23847-23858
23. Wedge MÈ, Naruzawa ES, Nigg M, Bernier L (2016) Diversity in yeast-mycelium dimorphism response of the Dutch elm disease pathogens: the inoculum size effect. Can J Microbiol 62:525-529
24. Wilson D, Fiori A, Brucker KD, Dijck PV, Stateva L (2010) *Candida albicans* Pde1p and Gpa2p comprise a regulatory module mediating agonist-induced cAMP signaling and environmental adaptation. Fungal Genet Biol 47:742-752
25. Yemelin A, Brauchler A, Jacob S, Laufer J, Heck L et al (2017) Identification of factors involved in dimorphism and pathogenicity of *Zymoseptoria tritici*. PLoS One 12:e0183065
26. Yin CM, Zheng LS, Zhu JH, Chen LG, Ma AM (2015) Enhancing stress tolerance by overexpression of a methionine sulfoxide reductase A (*Msr*A) gene in *Pleurotus ostreatus*. Appl Microbiol Biotechnol 99:3115-3126
27. Zhu HY, Liu DM, Wang YY, Ren DF, Zheng LS et al (2017) Use of the yeast-like cells of *Tremella fuciformis* as a cell factory to produce a *Pleurotus ostreatus* hydrophobin. Biotechnol Lett 39:1167-1173

28. Zhu HY, Yuan Y, Liu J, Zheng LS, Chen LG et al (2016) Comparing the sugar profiles and primary structures of alkali-extracted water-soluble polysaccharides in cell wall between the yeast and mycelial phases from *Tremella fuciformis*. J Microbiol 54:381-386

Figures

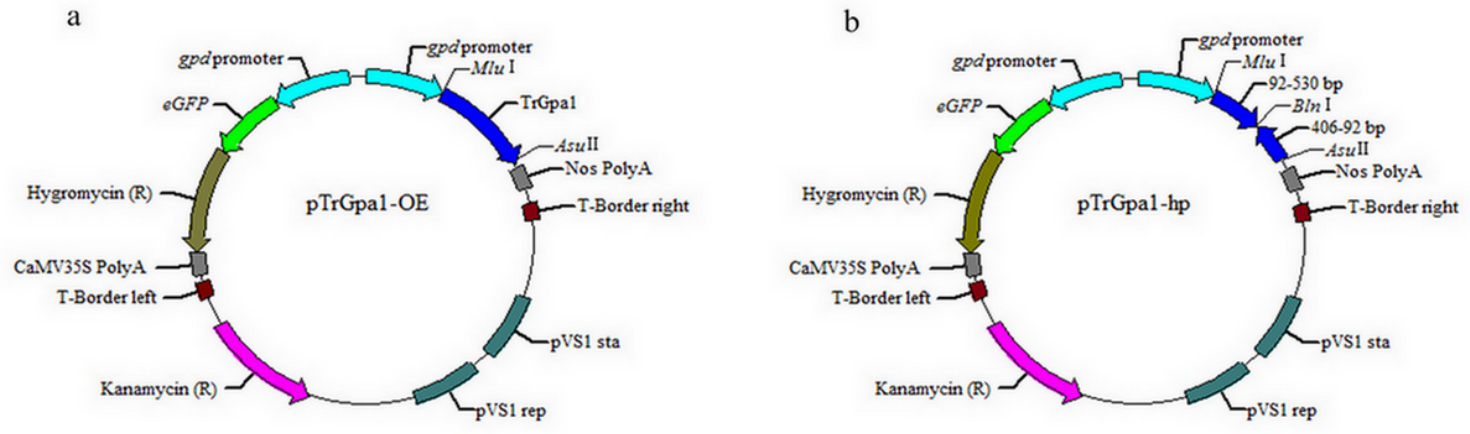

Figure 1

Map of the TrGpa1 over-expression vector (a) and knockdown vector (b).

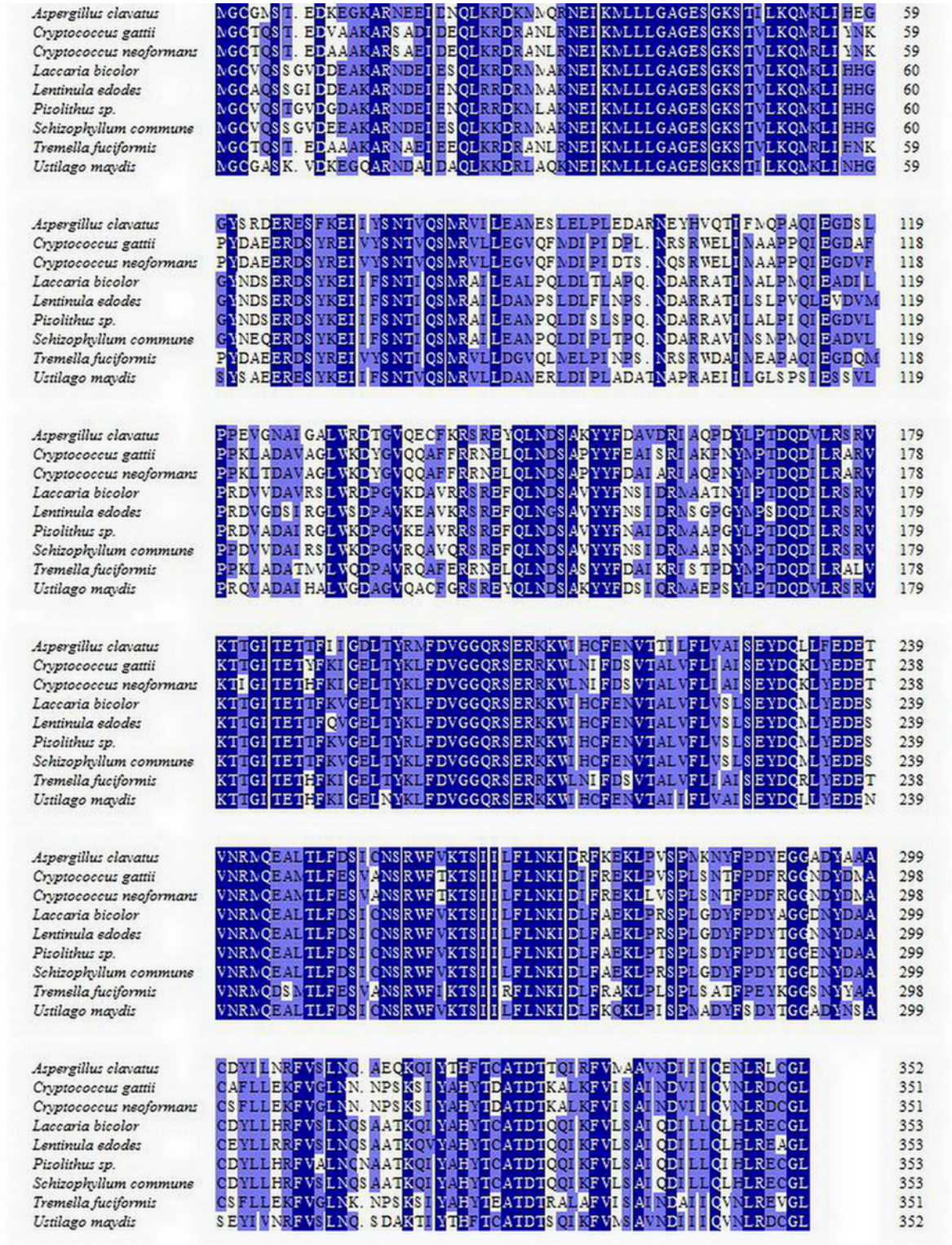

Figure 2

Multiple amino acid sequence alignment of TrGpa1 with homologues from other fungi: K. heveanensis (OCF36875.1), C. gattii (XP_003191999.1), C. neoformans (XP_566528.1), Pisolithus sp. (AAK15759.1), S. commune (XP_003029155.1), L. bicolor (XP_001888946.1), L. edodes (AAP13579.1), and H. marmoreus (KYQ31721.1). Conserved residues are shown in dark blue boxes, identical resides in light blue boxes, and

unrelated residues in a white bachground. Dots indicates gaps or the lack of a matching sequence of the protein sequences. Amino acid numbers are shown on the right.

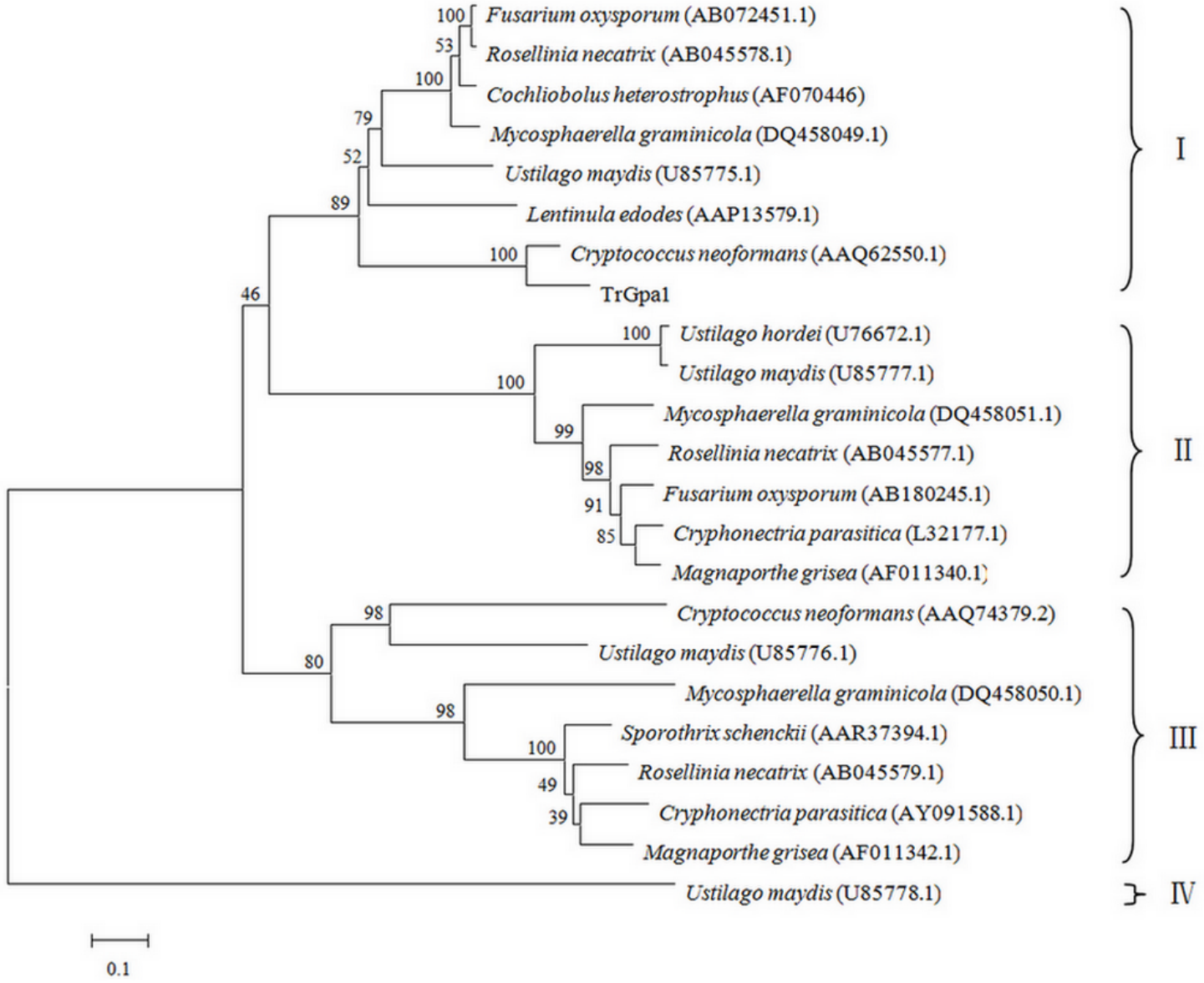

Figure 3

Phylogenetic tree of TrGpa1 was generated by the neighbor-joining (NJ) method using MEGA 6.0, based on the amino acid sequences of Gα proteins from 22 species. One thousand bootstrap replicates were calculated, and bootstrap values are shown at each node. The scale bar indicates an evolutionary distance of amino acid substitutions per position.

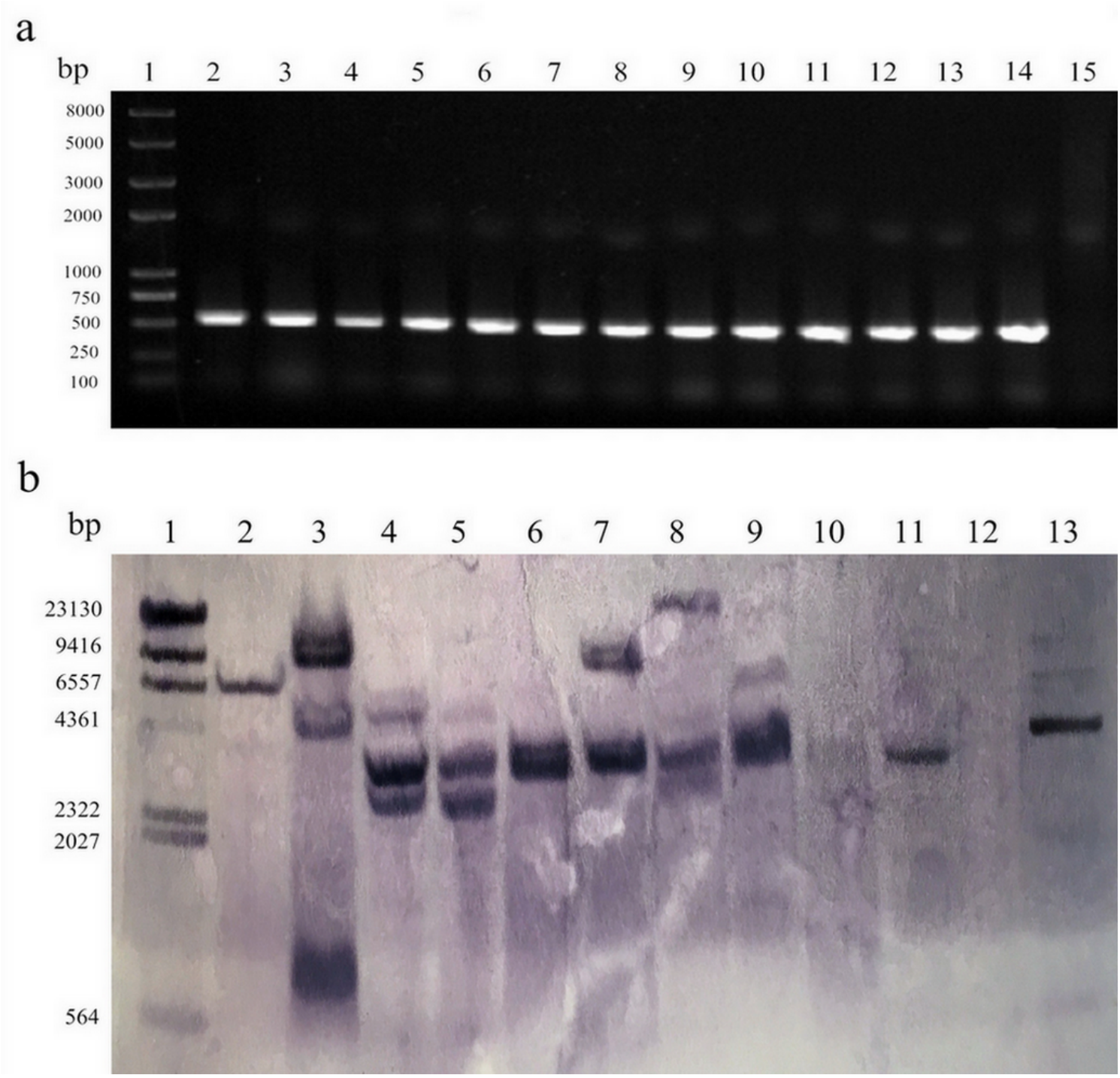

Figure 4

Stability test of the overexpression and knockdown transformants. a PCR assays of the egfp-hph in the transformants, plasmid pPEH-PH, and Y32. Lane 1, DNA marker. Lane 2-7, PCR products of overexpression transformants. Lane 8-13, PCR products of knockdown transformants. Lane 14, PCR product of pPEH-PH. Lane 15, PCR product of Y32. b Analysis of the integration of hph in T. fuciformis transformants by Southern blot. Genomic DNA digested with XhoI was probed using ~500 bp DIG-labeled egfp-hph. Lane 1, DNA marker. Lane 2-6, TrGpa1 overexpression transformants. Lane 7-11, TrGpa1

knockdown transformants. Lane 12, Y32. Lane 13, pPEH-PH. The molecular weight of DNA marker (bp) is shown on the left.

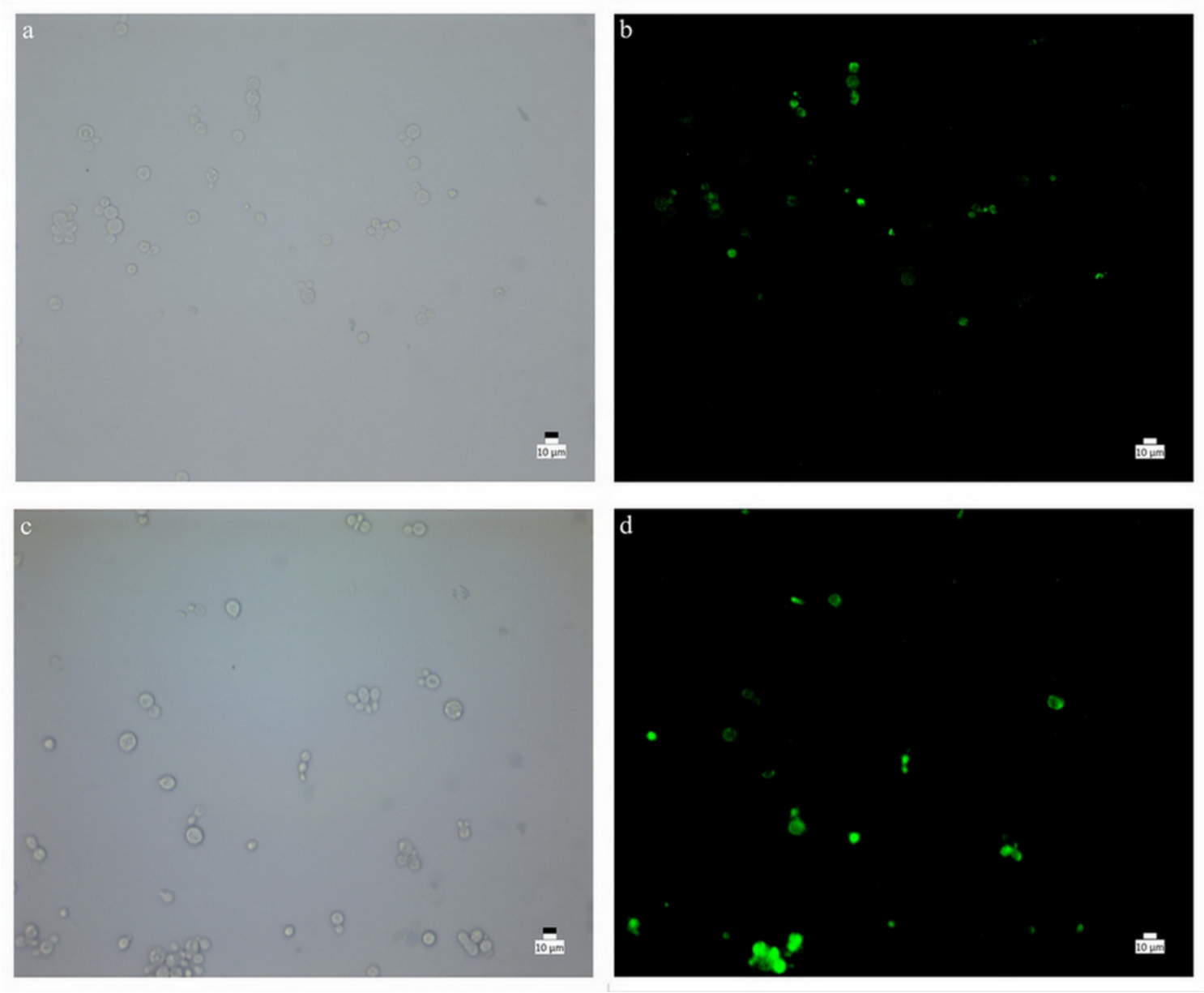

Figure 5

Detection for fluorescence under bright light (a overexpression transformant; c knockdown transformant) and corresponding UV light (b overexpression transformant; d knockdown transformant). Images were taken with 40 × fields of view, bar = 10 μm.

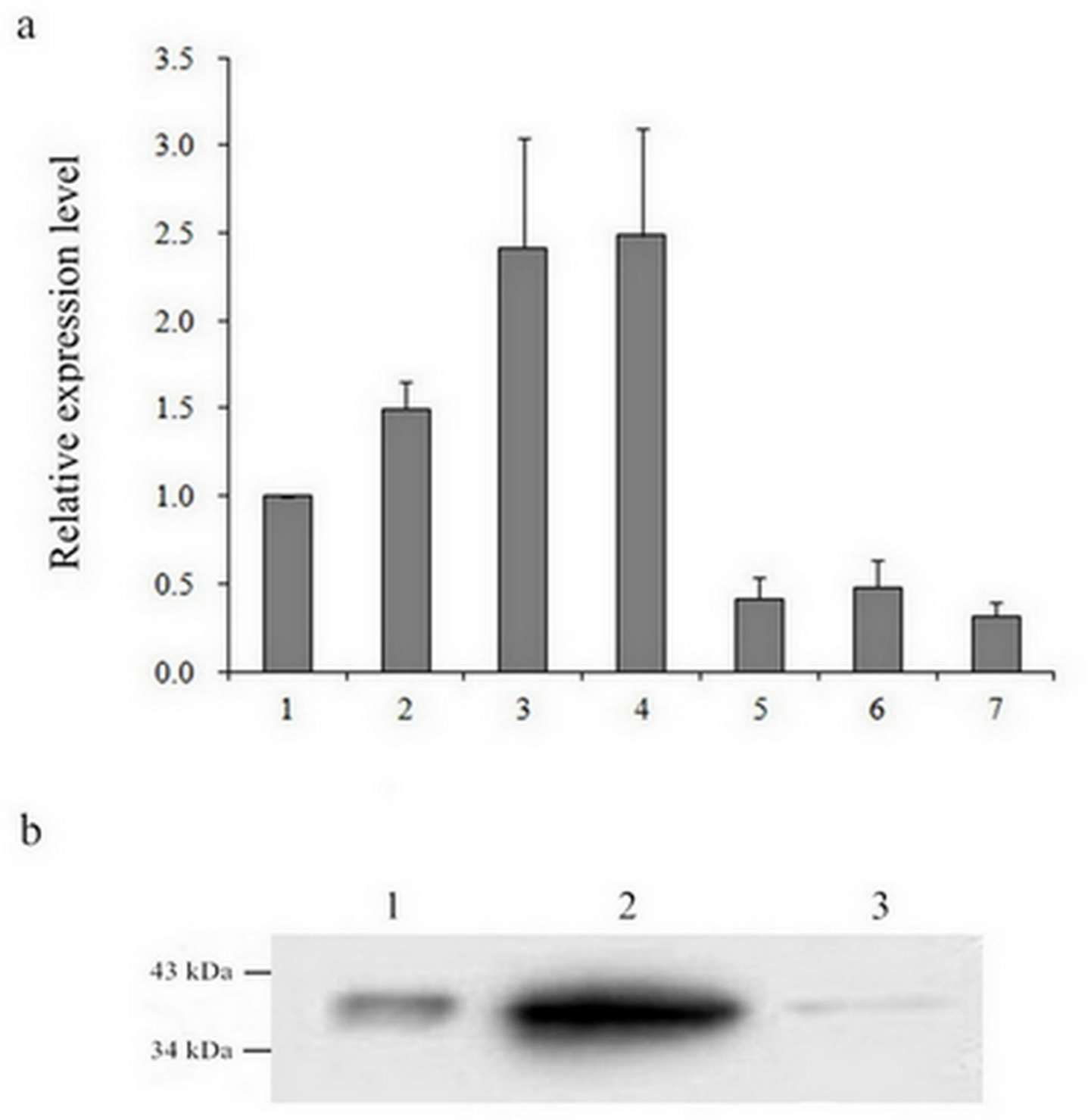

Figure 6

Gene expression analysis of transformants. a Relative expression levels of TrGpa1 in overexpression (2, 3, 4) and knockdown transformants (5, 6, 7) and Y32 (1). Data were presented as mean values of three replicates with the corresponding standard deviations. b Western blot analysis of Y32 (Lane 1), the overexpression transformant (Lane 2), and the knockdown transformant (Lane 3).

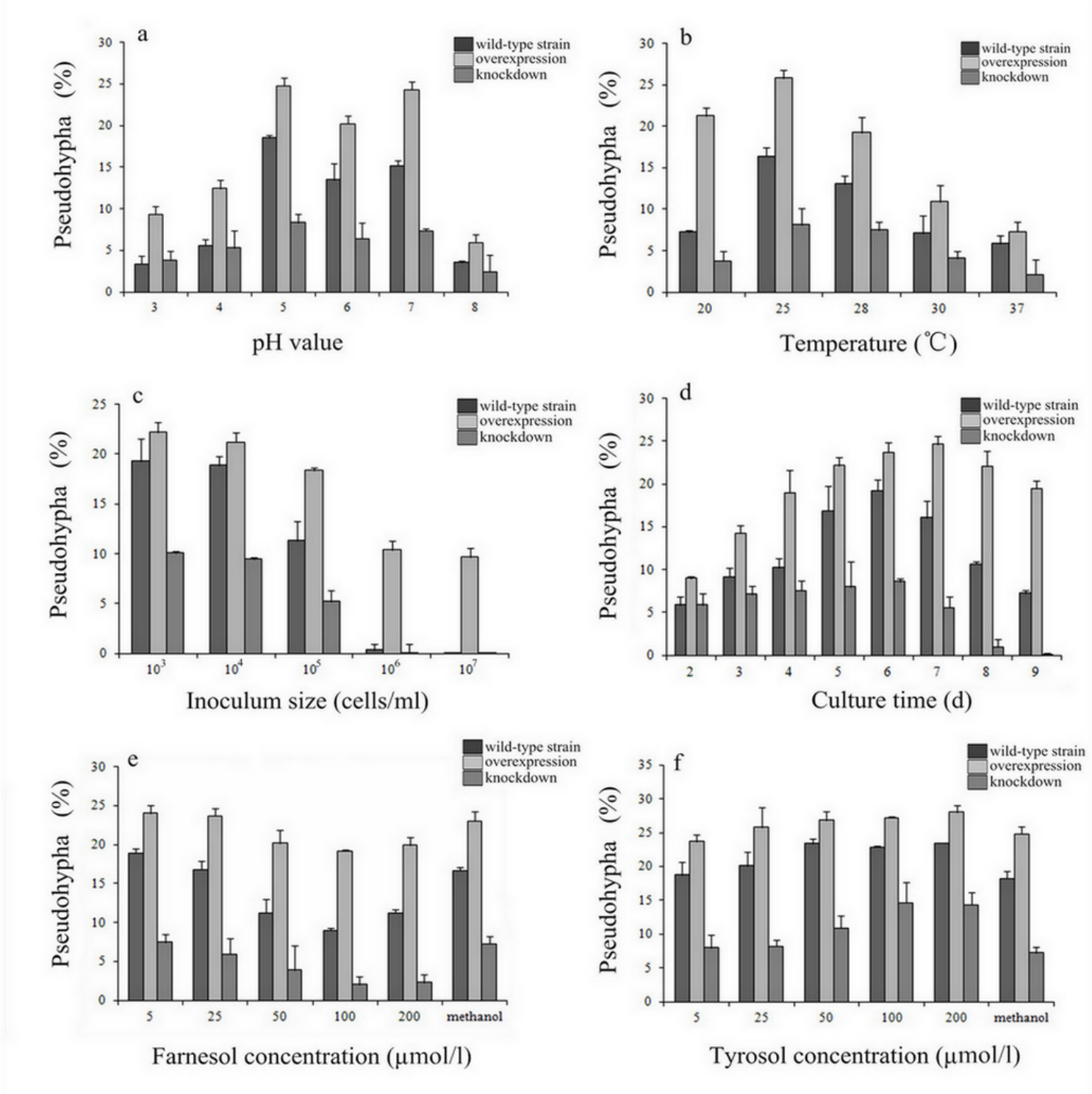

Figure 7

Effects of pH (a), temperature (b), culture time (c), inoculum size (d), farnesol (e) and tyrosol (f) on the phenotype of Y32, TrGpa1 overexpression transformant and knockdown transformant.